Taylor & Francis
Taylor & Francis Group

International Journal of Ambient Energy

ISSN: 0143-0750 (Print) 2162-8246 (Online) Journal homepage: www.tandfonline.com/journals/taen20

An effect of Joule heating and viscosity ratio on magnetic ferrohybrid nanofluid flow with entropy generation analysis

S.M. Sachhin, U.S. Mahabaleshwar , David Laroze & L. M. Pérez

To cite this article: S.M. Sachhin, U.S. Mahabaleshwar , David Laroze & L. M. Pérez (2026) An effect of Joule heating and viscosity ratio on magnetic ferrohybrid nanofluid flow with entropy generation analysis, International Journal of Ambient Energy, 47:1, 2663966, DOI: 10.1080/01430750.2026.2663966

To link to this article: https://doi.org/10.1080/01430750.2026.2663966

Published online: 07 May 2026.

INTERNATIONAL JOURNAL OF AMBIENT ENERGY
2026, VOL. 47, NO. 1, 2663966
https://doi.org/10.1080/01430750.2026.2663966

An effect of Joule heating and viscosity ratio on magnetic ferrohybrid nanofluid flow with entropy generation analysis

S.M. Sachhin [a], U.S. Mahabaleshwar[a], David Laroze[b] and L. M. Pérez[b,c]

[a]Department of Studies in Mathematics, Davangere University, Davangere, India; [b]Instituto de Alta Investigación, Universidad de Tarapacá, Arica, Chile; [c]Departamento de Ingeniería Industrial y de Sistemas, Universidad de Tarapacá, Arica, Chile

ABSTRACT

The current work aims to study the radiation and viscosity ratio influence on ferrohybrid nanofluid flow over an expanding surface with entropy generation analysis. There is a lack of study on ferrofluids in circumstance of the influence of Lorentz force and joule heating, heat dissipation, velocity slip with heat transfer and entropy analysis, and authors utilised the research gap. Governing equations are formulated to ordinary differential equations via similarity conversions, radiation, and heat generation terms included in the temperature equation and solved using Laguerrel polynomial and also calculated the entropy generation; several physical effects such as Brinkman number, magnetic field, inverse Darcy number, Radiation, Heat source/sink, Eckert number parameters are calculated and explained through graphs, and results of the current work illustrate that enhancing the mass transpiration slowdowns the velocity and increases the temperature, increasing the Eckert increases the temperature as well as entropy generation, increasing the magnetic field increases the temperature and reduces the velocity, and increasing the inverse Darcy number slowdowns the velocity profile and enhances the entropy generation to drag force. The present work using ferrohybrid nanofluid has many applications in aeronautical engineering as fluid rocket fuel, Biomedical fields such as medical resonance imaging and nanomedicine, among others.

Highlights

- Studied the magnetic field and viscosity ratio impact on the velocity of the flow.
- Fe_3O_4 and CuO nanoparticles are utilised to form ferrohybrid nanofluid.
- Laguerrel polynomial method utilised to solve the energy equation.
- Studied the entropy generation analysis with Joule heating.
- Engineering coefficients are calculated and explained through graphs.

ARTICLE HISTORY
Received 1 June 2024
Accepted 14 April 2026

KEYWORDS
Ferrohybrid nanofluid; Joule heating; viscosity ratio; entropy generation; thermal radiation; magnetic field

Nomenclature

List of symbols Descriptions SI unit

a	Stretching coefficient [s^{-1}]
A_1, A_2, A_3, A_4, A_5	Constants [–]
$K*$	Porous medium [m^2]
d	Stretching/shrinking term [–]
Ec	Eckert number [–]
$f(\eta)$	Velocity function [–]
Pr	Prandtl number [–]
C_p	Specific heat coefficient [$JK^{-1}Kg^{-1}$]
T_∞	Ambient temperature [K]
v_w	Wall velocity [ms^{-1}]
x, y	Coordinates [m]

Greek symbols

σ^*	Stephen Boltzmann constant [$Wm^{-2}K^{-4}$]
η	Similarity variable [–]
$\theta(\eta)$	Dimensionless Temperature [–]
k^*	Absorption coefficient [m^{-1}]

1. Introduction

With their unique magnetic and thermal properties combination, ferrohybrid nanofluids are finding innovative applications across various engineering fields. For instance, chemical engineering enhances mass transfer processes, while electrical and electronics engineering is crucial for developing advanced sensors and cooling systems for electronic devices. This domain's ongoing research and development suggest a promising future for ferrohybrid nanofluids in technological advancements. The permeable stretching surface was used by Mansourian, Dinarvand, and Pop (2022) to study the behaviour of ferrohybrid nanofluid flow. Syam Sundar et al. (2017) studied the synthesis of ferro nanofluids using the chemical co-precipitation method. Mehrali et al. (2017) explored the permanent magnetic field influence on laminar ferro-graphene nanofluid movement with

CONTACT S.M. Sachhin sachinsm030@gmail.com; U.S. Mahabaleshwar u.s.m@davangereuniversity.ac.in

heat transfer. Yang et al. (2020) studied the effect of friction drag and heat transfer in ferrite nanoparticles due to the existence of the Curie temperature in ferromagnetic fluid flows. Liu et al. (2019) investigated the effects of the magnetic field produced by assembling ferrite nanoparticle electromagnets. Ferroxidase and carbon nanotubes were used by Qureshi et al. (2023) to study the influence of thermal performance on hybrid nanofluid.

The Viscosity ratio is a non-dimensional quantity that has a crucial role in the examination of heat conduction from a wall to a moving fluid, particularly in the field of polymer extrusion. The viscosity ratio utility extends to various engineering disciplines, offering insights into the complex dynamics of fluid movement and energy transfer. Analytical formulations utilised by Dukhan, Al-Rammahi, and Suleiman (2013) to study the influence of the Darcy-Brinkman model on the velocity of the fluid. The viscosity ratio impact on fluid motion over an expanding sheet was calculated by Minale (2016). Shear stress over the cell surface was studied by Yao, Shen, and Ding (2013) by using the effect of the Brinkman number via interstitial fluid flow. Nield (1983), Bèg, Takhar, and Soundalgekar (1998), and Tsay and Weinbaum (1991) studied the impact of the Brinkman ratio on three-dimensional fluid flow over a square array of circular cylindrical pipes.

Entropy generation in fluid flow applications is a critical aspect of thermodynamics that deals with the irreversibility of processes and the efficiency of energy conversion. It is particularly significant in the optimisation and design of science and engineering fields, such as microchannel heat transformers, where minimising entropy can lead to more efficient operations. Shojaeian and Koşar (2014) explored the convective heat movement and entropy production in Newtonian fluid movements between parallel sheets using isothermal boundary conditions. Singh et al. (2010) researched entropy generation analysis with heat transfer in hybrid nanofluids. Srinivasacharya and Hima Bindu (2016) studied the entropy generation on micropolar fluid motion via inclined parallel plates with zero pressure gradients. Sarma and Mondal (2018) explored the entropy for the motion of a viscoelastic fluid via a parallel microchannel with an applied pressure gradient. Huminic and Huminic (2020) and Shah et al. (2019) studied the impact of entropy generation on hybrid nano fluids in the different forms of thermal radiations for various boundaries and physical conditions.

Magnetic fields have a significant impact on fluid flow, offering a variety of applications across different industries. For instance, magnetorheological fluids can often change their viscosity with a magnetic field, which is beneficial for creating adaptive shock absorbers and clutches. Cunha and Sobral (2004) studied the impact of the magnetic droplet's freely moving on fluid flow. Li and Xuan (2009) worked on the convective heat transport in an aqueous magnetic fluid moving via a thin wire in the external magnetic field. Radionov, Podoltsev, and Zahorulko (2012) created a mathematical model for the nonlinear magnetic characteristics of the materials used in the magnetic core and shaft. Kumar et al. (2022) and Li et al. (2007) concentrated on an electrically nonconductive and incompressible fluid with magnetisation and a low Curie temperature.

Joule heating is a functional process in which the electric current passing through a conductor emits heat. This phenomenon has significant applications in fluid flow, particularly in microfluidic devices where precise temperature control is crucial. For instance, in magnetohydrodynamic (MHD) flows, Joule heating can influence fluid properties and flow patterns. The wire coating technique was used by Khan et al. (2020) to study the viscoelastic Eyring fluid with the impact of magnetohydrodynamics. Hayat, Shafiq, and Alsaedi (2014) explored the impact of dissipation on third-grade fluid movement. Numerical methods were used by Erickson, Sinton, and Li (2003) and Tang et al. (2004) to examine the Joule heating influence on the electroosmotic motion, which is used in capillary electrophoresis. Sridharan et al. (2011) and Zhao and Yang (2012) studied the effect of joule heating to control the performance of capillary electrophoresis in terms of induced heat flow for electroosmotic movement.

Radiation effects on fluid flow have significant implications in various applications, particularly in the context of non-Newtonian fluids used in industrial and technological processes. Water-based carbon nanotubes were used by Yu and Wang(2022) to study the heat and fluid motion over two expanding rotating disks. Pramanik (2014) investigates the movement of a non-Newtonian fluid with energy transfer via an expanding surface. Thermal radiation effects on the movement of micropolar fluid and energy transfer were explored by Bhattacharyya et al. (2012). Megahed, Reddy, and Abbas (2021) examine the issue of heat transmission and boundary-layer laminar motion for MHD fluid caused by an unstable expanded surface with stretched heat flux. Klazly and Bognár (2022) examine the effective viscosity impact on fluid flow. Bognár (2012) examines the phenomena of heat transport using power law fluids. Mahabaleshwar et al. (2024), Sachhin et al. (2025), Sachhin et al. (2025) and Sachhin et al. (2025) investigate the movement of fluid with heat transfer via an expanding surface. E. Cuce, Guclu, and Cuce (2020), E. Cuce et al. (2020) and A. CÜCE, GÜÇLÜ, and Cuce (2022) studied the application of nanofluids through a mini-channel heat sink, optimising the coefficient of performance (COP) and enhancing the heat transfer capabilities of TECs, considering the effects of viscosity and nonuniform heat generation studied by Yusuf (2023), Khan et al. (2023), Yusuf (2024), Salawu et al. (2023) and Mabood, Yusuf, and Bognár (2020). Sachhin et al. (2024) explored the micropolar fluid flow with heat transfer. Ali et al. (2023) and Ali et al. (2019) studied the enhanced heat transfer on peristaltic flow of nanofluid with heat flux effects. Influence of entropy generation on hybrid nano fluids in the various forms of thermal radiations for various boundaries and physical conditions studied by Hussain et al. (2023), Mumraiz et al. (2021), Awais et al. (2021), Awais et al. (2018), Yih (1999), Sachhin et al. (2026), Barna et al. (2020) and Lone et al. (2023).

Motivated by the above research and applications, the current work examines the influence of magnetic field and viscosity ratio on ferrohybrid nanofluid movement over an expanding surface with entropy generation. Fe3O4 and CuO nanoparticles are mixed in a base fluid to form a ferrohybrid nanofluid. There is a lack of study on ferrofluids in the circumstance of dissipation and magnetic field with energy transfer and entropy generation; the authors utilised the research gap. radiation, and heat generation terms included in the temperature equation and solved using Laguerrel polynomial, and also calculated the entropy generation, several physical effects such as Brinkman number, magnetic field, inverse Darcy number, Radiation, Heat source/sink, Eckert number are examined. The present work using ferrohybrid nanofluid has many applications in aeronautical engineering as fluid rocket fuel, Biomedical fields such as medical resonance imaging, drug delivery, and nanomedicine, among others.

1.1. The research gaps addressed by the current analysis

The following are the research gaps addressed by the current analysis:

- Hybrid nanoparticles are considered with the viscosity ratio and the magnetic field impact on ferrofluid flow across porous media.
- Considered Newtonian, incompressible laminar flow.
- examined the analysis of entropy generation.
- Solar radiation, heat generation, and viscous dissipation are considered.
- Neglected concentration and chemical reaction.
- Neglected pressure gradient i.e. $\nabla p = 0$.
- Considered velocity slip boundary conditions.
- Considered steady flow i.e. $\frac{\partial u}{\partial t} = 0$.

The percentage upsurge in the physical quantities due to the hybrid nanoparticles is compared to hybrid and single nanoparticles in a water hybrid nanofluid with velocity slip boundary conditions.

2. Mathematical formulation

The two-dimensional electromagnetic ferrohybrid nanofluid motion is considered over the porous sheet. Two nanoparticles, Cuo and Fe_3O_4, immersed in the conventional fluid water whose thermophysical characteristics are stated in Table 1. Several physical parameters such as solar radiation, joule heating, viscosity ratio, and viscous dissipation are employed to study phenomena. Considered the Cartesian coordinate system, which shows the x-axis portrays the direction of movement towards the sheet and the y-axis portrays the normal to the surface movement. Magnetic fields are perpendicularly applied to the fluid motion, and the sheet has a stretching velocity of $u = ax = u_w$. When $u = 0$it gives ambient fluid velocity. T_w and T_∞ are fluid and ambient temperature. Figure 1(a) represents the schematic represents of the fluid movement; Figure 1(b) represents the real-world applications of ferrohybrid nanofluid.

2.1. Modelling assumptions and justification of single-phase model

For the current study, a single-phase model is adopted to depict the ferrohybrid nanofluid. The model considers that the nanoparticles and base fluid have similar temperature and velocity, thus, no slip between the phases is allowed. Since the nanoparticle volume fractions are very low, it is reasonable to neglect Brownian diffusion and thermophoresis.

Besides that, the movement is considered to be steady, laminar, and incompressible, and the nanoparticles, along with the base fluid, are evenly dispersed without forming clusters. Under such circumstances, the effective thermophysical characteristics of the ferrohybrid nanofluid can be accurately determined through the use of a conventional mixture. In the literature, the single-phase model is the most common one, especially in boundary-layer MHD nanofluid experiments where nanoparticle migration effects are minimal. Hence, this model offers a very good macroscopic description of the movement of a ferrohybrid nanofluid across an expanding sheet with a magnetic field and entropy generation.

Table 1. Ferrohybrid nanofluid thermophysical properties (Mansourian, Dinarvand, and Pop (2022); Syam Sundar et al. 2017; Mehrali et al. 2017; Liu et al. 2019; Yang et al. 2020; Qureshi et al. 2023).

Properties	H_2O	Fe_3O_4	CuO
σ	0.05	250	0.4
ρ	997.1	5180	6510
C_p	4179	670	540
κ	0.613	9.7	18

Continuity equation is considered as (Dukhan, Al-Rammahi, and Suleiman (2013) and Li and Xuan (2009))

$$\nabla \bullet \vec{q} = 0, \tag{a}$$

The velocity equation is considered as (Dukhan, Al-Rammahi, and Suleiman (2013) and Li and Xuan (2009))

$$\left[\left(\vec{q} \bullet \nabla\right)\vec{q}\right] = \frac{\mu_{eff}}{\rho_{hnf}}\nabla^2\vec{q} - \frac{\nu_{hnf}}{K*}\vec{q} - \frac{\sigma_{hnf}}{\rho_{hnf}}\left(B_0^2\vec{q}\right), \tag{b}$$

Vector form of temperature equation (Dukhan, Al-Rammahi, and Suleiman (2013) and Li and Xuan (2009)).

$$(\rho C_p)_{hnf}\left[\left(\vec{q} \bullet \nabla\right)T\right] = \kappa_{hnf}\nabla^2 T - \nabla q_r + Q(T - T_\infty) + \mu_{hnf}\left(\nabla\vec{q}\right)^2 + \sigma_{hnf}\left(\vec{q}B_0\right)^2, \tag{c}$$

where $\vec{q} = (u, v)$ is the velocity vector, T is the temperature.

The governing equations for the problem are obtained as (Dukhan, Al-Rammahi, and Suleiman (2013), Li and Xuan (2009), Hayat, Shafiq, and Alsaedi (2014) and Pramanik (2014)).

- Continuity equation

$$\frac{\partial u}{\partial x} + \frac{\partial v}{\partial y} = 0, \tag{1}$$

- Velocity equation

$$u\frac{\partial u}{\partial x} + v\frac{\partial u}{\partial y} = \frac{\mu_{eff}}{\rho_{hnf}}\frac{\partial^2 u}{\partial y^2} - \frac{\sigma_{hnf}}{\rho_{hnf}}B_0^2 u - \frac{\mu_{hnf}}{\rho_{hnf}K*}u, \tag{2}$$

- Temperature equation

$$u\frac{\partial T}{\partial x} + v\frac{\partial T}{\partial y} = \frac{\kappa_{hnf}}{(\rho C_p)_{hnf}}\frac{\partial^2 T}{\partial y^2} - \frac{1}{(\rho C_p)_{hnf}}\frac{\partial q_r}{\partial y} + \frac{Q_0(T - T_\infty)}{(\rho C_p)_{hnf}} + \frac{\mu_{hnf}}{(\rho C_p)_{hnf}}\left(\frac{\partial u}{\partial y}\right)^2 + \frac{\sigma_{hnf}}{(\rho C_p)_{hnf}}(uB_0)^2, \tag{3}$$

μ_{eff} is the effective viscosity, ρ denotes density, μ is the dynamic viscosity, κ is the thermal conductivity, σ is the electrical conductivity, and T is the temperature, q_r is the radiative heat flux, B_0 denotes the magnetic strength.

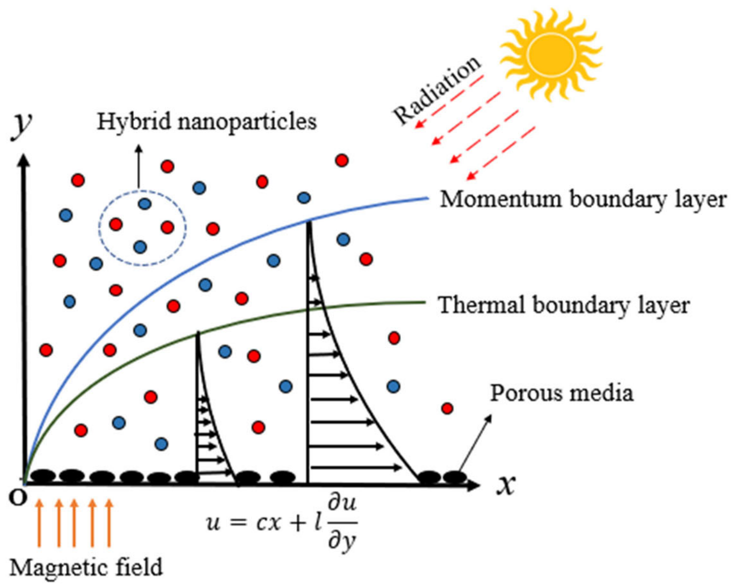

(a): Schematic diagram.

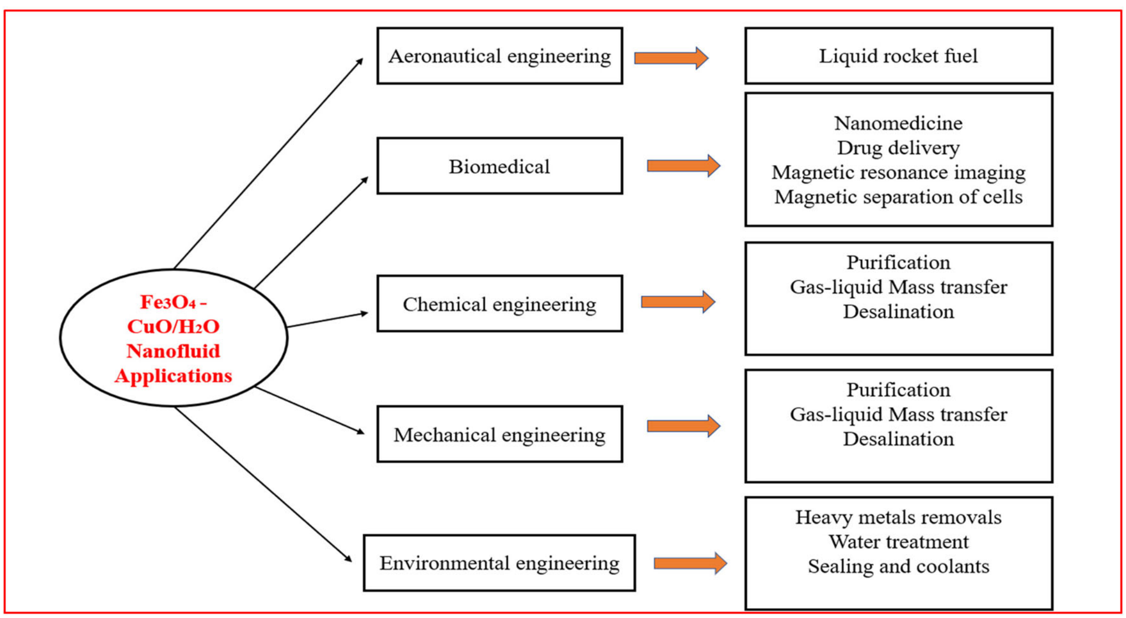

(b): Real-world applications of Ferro-hybrid nanofluid.

Figure 1. (a) Schematic diagram and (b) real-world applications of ferrohybrid nanofluid.

Boundary conditions considered as Dukhan, Al-Rammahi, and Suleiman (2013), Li and Xuan (2009), Hayat, Shafiq, and Alsaedi (2014) and Pramanik (2014).

$$
\begin{aligned}
&u = cx + l\frac{\partial u}{\partial y},\ v = v_w,\ T = T_w(x) = T_\infty + b\left(\tfrac{x}{l}\right)^2, \text{ at } y = 0.\\
&u = 0, \qquad v = 0, \quad T \to T_\infty, \qquad\qquad \text{as } y \to \infty
\end{aligned} \tag{4}
$$

2.2. Physical interpretation of boundary conditions

The boundary conditions considered in the current work are those of a physically realistic stretching sheet scenario that arises naturally in polymer extrusion and coating operations.

At the wall ($y = 0$):

- The stretching velocity $u = cx + l\frac{\partial u}{\partial y}$ stands for a linearly stretching surface, where $c > 0$ means a positive value of the stretching rate. This scenario is typical of polymer sheet extrusion, wire coating, and glass fibre manufacturing processes.
- The normal velocity $v_w$signifies to the surface mass transpiration. In the event that $v_w < 0$, the suction occurs which stabilises the boundary layer by drawing the fluid towards the sheet. In the case of $v_w > 0$, the injection (blowing) happens that results in the boundary-layer thickening.
- The velocity slip condition implies that the fluid velocity at the wall is slightly different from the sheet velocity. This condition is significant in micro-scale flows, rarefied gases, and

nanofluid contexts where the no-slip assumption might not hold.

- The wall temperature T_w is taken constant, thus the surface is an isothermal stretching one kept at a certain temperature.

At the surface an infinite distance away ($y \to \infty$):

- The fluid velocity tends to zero which means the stretching effect becomes negligible at large distances from the sheet.
- The temperature tends to the ambient temperature T_∞ thus the thermal boundary layer disappears asymptotically.

Taken together, these boundary conditions describe a steady, two-dimensional ferrohybrid nanofluid due to a permeable expanding surface under combined magnetic and thermal effects.

Radiative heat flux is determined as Pramanik (2014) and Bhattacharyya et al. (2012).

$$q_r = \frac{4\sigma * T_\infty^3}{3k*}\frac{\partial T^4}{\partial y}, \tag{5}$$

$\Rightarrow \frac{\partial q_r}{\partial y} = -\frac{16\sigma * T_\infty^3}{3k*}\frac{\partial^2 T}{\partial y^2}$, where $T^4 = (4T - 3T_\infty)T_\infty^3$, we utilised the given set of similarity terms to translate the given equation to dimensionless (Dukhan, Al-Rammahi, and Suleiman (2013), Li and Xuan (2009), Hayat, Shafiq, and Alsaedi (2014) and Pramanik (2014)).

$$u = axf'(\eta), \qquad v = -f(\eta)\sqrt{a\nu_f},$$
$$T(\eta) = T_\infty + \Delta T\theta(\eta), \quad \eta = y\sqrt{\frac{a}{\nu_f}}, \qquad \Delta T = T_w - T_\infty. \tag{6}$$

Adding Equations (5)–(3) gives

$$u\frac{\partial T}{\partial x} + v\frac{\partial T}{\partial y} = \left(\frac{\kappa_{hnf}}{(\rho C_p)_{hnf}} + \frac{1}{(\rho C_p)_{hnf}}\frac{16\sigma^* T_\infty^3}{3k^*}\right)\frac{\partial^2 T}{\partial y^2} + \frac{Q_0(T - T_\infty)}{(\rho C_p)_{hnf}} + \frac{\mu_{hnf}}{(\rho C_p)_{hnf}}\left(\frac{\partial u}{\partial y}\right)^2 + \frac{\sigma_{hnf}}{(\rho C_p)_{hnf}}(uB_0)^2, \tag{7}$$

By using Equation (6), the modified governing equations formulated as

$$\Lambda\frac{d^3 f}{d\eta^3} + A_2 f(\eta)\frac{d^2 f}{d\eta^2} - A_2\left(\frac{df}{d\eta}\right)^2 - A_3 M\frac{df}{d\eta} - A_1 Da^{-1}\frac{df}{d\eta} = 0, \tag{8}$$

$$\chi_1\frac{d^2\theta}{d\eta^2} + A_5\left(f(\eta)\frac{d\theta}{d\eta} - 2\frac{df}{d\eta}\theta(\eta)\right) + Ni\theta(\eta) + Ec\left[A_1\frac{d^2 f}{d\eta^2} + A_3 M\left(\frac{df}{d\eta}\right)^2\right] = 0, \tag{9}$$

Where $A_1 = \frac{\mu_{hnf}}{\mu_f}, A_2 = \frac{\rho_{hnf}}{\rho_f}, A_3 = \frac{\sigma_{hnf}}{\sigma_f}, A_4 = \frac{\kappa_{hnf}}{\kappa_f}, A_5 = \frac{(\rho C_p)_{hnf}}{(\rho C_p)_f}$ are constants. $M = \frac{\sigma_f B_0^2}{a\rho_f}$ is the magnetic parameter, $Nr = \frac{16\sigma * T_\infty^3}{3\kappa_f k*}$ is the thermal radiation, $Ni = \frac{Q_0}{a(\rho C_p)_f}$ is the heat source/sink parameter, Pr $\left(= \frac{\mu_f (C_p)_f}{\kappa_f}\right)$ is the Prandtl number, $S\left(= -\frac{v_w}{\sqrt{a\nu_f}}\right)$ is the mass transpiration. $\chi_1 = \frac{(A_4 + Nr)}{\Pr}$. $Da^{-1} = \frac{\nu_f}{K*a}$ is the inverse Darcy number. Modified boundary conditions for the flow problem (Dukhan, Al-Rammahi, and Suleiman 2013; Li and Xuan 2009; Hayat, Shafiq, and Alsaedi 2014; Pramanik 2014).

$$f(0) = S, \quad f'(0) = d + Lf''(0), \quad \theta(0) = 1, \quad at \quad \eta = 0,$$
$$\theta(\infty) = 0, \quad f'(\infty) = 0, \qquad as \quad \eta \to \infty. \tag{10}$$

2.3. Analytic solution for velocity equation

By boundary condition Equation (10), we calculate the solution for Equation (8) as follows (Dukhan, Al-Rammahi, and Suleiman 2013; Li and Xuan 2009; Hayat, Shafiq, and Alsaedi 2014; Pramanik 2014).

$$f(\eta) = S + d\frac{1 - e^{-\beta\eta}}{\beta(1 + L\beta)}. \tag{11}$$

By using the above equation, we solve Equation (8) and obtain the algebraic solution as follows

$$(L\Lambda)\beta^3 + (\Lambda - A_2 SL)\beta^2 - (A_3 ML\beta + A_2 S + A_1 Da^{-1}L)\beta - (A_2 d + A_3 M + A_1 Da^{-1}) = 0, \tag{12}$$

The above equation is rewritten as

$$\xi_1\beta^3 + \xi_2\beta^2 + \xi_3\beta + \xi_4 = 0, \tag{13}$$

where

$$\xi_1 = L\Lambda, \qquad \xi_3 = A_3 ML\beta + A_2 S + A_1 Da^{-1}L,$$
$$\xi_4 = A_2 d + A_3 M + A_1 Da^{-1}, \quad \xi_2 = \Lambda - A_2 SL. \tag{14}$$

All possible roots of the above Equation (13) are given as

$$\beta_1 = \frac{-\frac{\xi_2}{3\xi_1} - (2^{1/3}(-\xi_2^2 + 3\xi_1\xi_3))}{3\xi_1\left(z + \sqrt{4(-\xi_2^2 + 3\xi_1\xi_3)^3 + (z)^2}\right)^{1/3}} + \frac{1}{3\ 2^{1/3}\xi_1}\left(z + \sqrt{4(-\xi_2^2 + 3\xi_1\xi_3)^3 + (z)^2}\right)^{1/3},$$

$$\beta_2 = \frac{-\frac{\xi_2}{3\xi_1} + \left((1 + i\sqrt{3})(-\xi_2^2 + 3\xi_1\xi_3)\right)}{3\ \xi_1 2^{1/3}\left(z + \sqrt{4(-\xi_2^2 + 3\xi_1\xi_3)^3 + (z)^2}\right)^{1/3}} - \frac{1}{6\xi_1 2^{1/3}}(1 + i\sqrt{3})\left(z + \sqrt{4(-\xi_2^2 + 3\xi_1\xi_3)^3 + (z)^2}\right)^{1/3},$$

$$\beta_3 = \frac{-\frac{\xi_2}{3\xi_1} + \left((1 + i\sqrt{3})(-\xi_2^2 + 3\xi_1\xi_3)\right)}{3\ \xi_1 2^{1/3}\left(z + \sqrt{4(-\xi_2^2 + 3\xi_1\xi_3)^3 + (z)^2}\right)^{1/3}} + \frac{1}{6\xi_1 2^{1/3}}(1 + i\sqrt{3})\left(z + \sqrt{4(-\xi_2^2 + 3\xi_1\xi_3)^3 + (z)^2}\right)^{1/3} \tag{15}$$

where

$$z = (-2\xi_2^3 + 9\xi_1\xi_2\xi_3 - 27\xi_1^2\xi_4).$$

2.4. Exact solution of the temperature equation

We chose variable t to solve Equation (9) as follows (Mansourian, Dinarvand, and Pop 2022; Dukhan, Al-Rammahi, and Suleiman 2013; Li and Xuan 2009):

$$t = -e^{-\beta\eta}, \tag{16}$$

by using Equation (16), the energy equation is calculated as

$$t\frac{\partial^2\theta}{\partial t^2} + (1 - \xi_5 S - \xi_5 t)\frac{\partial\theta}{\partial t} + \xi_5\frac{Ni_1}{t}\theta(\eta) = -\xi_5 Ec_1 t \tag{17}$$

where

$$\xi_5 = -\frac{A_4 S}{\chi_1\beta^2(1+L\beta)}, \quad Ni_1 = \frac{Ni}{A_5\beta(1+L\beta)},$$
$$Ec_1 = Ec\left(\frac{-A_1 d^2}{\xi_5(1+L\beta)^2} - \frac{A_3 M d^2}{\xi_5\beta^2(1+L\beta)^2}\right). \tag{18}$$

Modified B. Cs are Dukhan, Al-Rammahi, and Suleiman (2013), Li and Xuan (2009), Hayat, Shafiq, and Alsaedi (2014) and Pramanik (2014).

$$\theta(t=-1) = 1, \quad \theta(t=0) = 0. \tag{20}$$

Equations (17) and (20) solved as

$$\theta(t) = (1 - B_3)(-t)^{B_2}\frac{L[2-B_2, B_1, \xi_5 t]}{L[2-B_2, B_1, -\xi_5]} + B_3 t^2, \tag{21}$$

$L[a, b, z]$ is the generalised Laguerre polynomials; B_1, B_2, and B_3 are as follows:

$$B_1 = \sqrt{\xi_5{}^2 S^2 + 4\xi_5 Ni_1}, \quad B_2 = \frac{\xi_5 S + B_1}{2}, \quad \text{and}$$
$$B_3 = \frac{\xi_5 Ec_1}{\xi_5(Ni_1 + 2S) - 4}, \tag{22}$$

Here, the wall temperature gradient is calculated as

$$\theta'(0) = \beta\left(B_3(B_2 - 2) - B_2 + \frac{\xi_5(1-B_3)}{(B_1+1)}\frac{L[1-B_2, B_1+1, -\xi_5]}{L[2-B_2, B_1, -\xi_5]}\right). \tag{23}$$

2.5. Analytical approach and methodology algorithm

The main steps to get an analytical solution are as follows:

- The considered Equations (2) and (3) are converted to nonlinear ODEs with the help of similarity transformations.
- The formulated nonlinear differential Equations (8) and (9) with boundary restrictions (10) are elucidated by the Analytical approach.
- Equation (11) was obtained by calculating the boundary condition Equation (10).
- Using Equation (10), we calculated the solution for Equation (8), by differentiating the solution $f(\eta)$and gained cubic polynomials (12) having three roots.
- By using a variable $t = -e^{-\beta\eta}$ solved the temperature equations and obtained Equation (17). Later solved by using a Laguerrel polynomial, which obtained the solutions for temperature.

2.6. Physical quantities or engineering quantities

Skin friction and Nusselt numbers can be calculated as follows (Dukhan, Al-Rammahi, and Suleiman 2013, Li and Xuan 2009, Hayat, Shafiq, and Alsaedi 2014; Pramanik 2014):

$$C_f = \frac{2\tau_w}{\rho_{hnf}u_w^2} \Rightarrow C_f\frac{\sqrt{Re_x}}{2} = -\frac{A_1}{A_2}f''(0), \tag{23}$$

$$Nu = \frac{xq_w}{\kappa_f(T_w - T_\infty)} \Rightarrow \frac{Nu}{\sqrt{Re_x}} = -A_4\theta'(0), \tag{24}$$

$Re_x = \frac{ax^2}{\nu_f}$ denotes the local Reynolds number. Wall shear stress $\tau_w = \mu_{hnf}\left(\frac{\partial u}{\partial y}\right)_{y=0}$, heat flux of the surface $q_w = -\kappa_{hnf}\left(\frac{\partial T}{\partial y}\right)_{y=0}$.

2.7. Solution for entropy generation

The considered entropy equation is defined as follows Shojaeian and Koşar (2014), Singh et al. (2010), Srinivasacharya and Hima Bindu (2016), Sarma and Mondal (2018), Huminic and Huminic (2020) and Shah et al. (2019):

$$Sg = \frac{\kappa_f}{T_\infty^2}\left[A_4 + \frac{16\sigma * T_\infty^3}{3k * \kappa_f}\right]\left(\frac{\partial T}{\partial y}\right)^2 + \frac{\mu_{hnf}}{T_\infty}\left(\frac{\partial u}{\partial y}\right)^2 + \frac{\sigma_{hnf}}{T_\infty}(uB_0)^2 + \frac{\mu_{hnf}}{T_\infty K*}u^2, \tag{25}$$

$$\text{Energy loss via heat transfer} \Rightarrow \frac{\kappa_f}{T_\infty^2}\left[A_4 + \frac{16\sigma * T_\infty^3}{3k * \kappa_f}\right]\left(\frac{\partial T}{\partial y}\right)^2,$$
$$\text{Energy loss via fluid friction} \Rightarrow \frac{\mu_{hnf}}{T_\infty}\left(\frac{\partial u}{\partial y}\right)^2,$$
$$\text{Energy loss via Joule heating and porosity} \Rightarrow \frac{\sigma_{hnf}}{T_\infty}(uB_0)^2 + \frac{\mu_{hnf}}{T_\infty K*}u^2, \tag{26}$$

By solving the above equation, we obtain

$$Ng = (A_4 + Nr)\delta(\theta')^2 + Br[A_1(f'')^2 + A_3 M(f')^2 + A_1 Da^{-1}(f')^2], \tag{27}$$

where $Br = Ec \times \Pr$, $\delta = \frac{T_w - T_\infty}{T_\infty}$.

- Dynamic viscosity given as

$$\frac{\mu_{hnf}}{\mu_f} = \frac{1}{(1-\phi_1)^{2.5}(1-\phi_2)^{2.5}},$$

- Density of the hybrid nanofluid quantity as follows:

$$\frac{\rho_{hnf}}{\rho_f} = (1-\phi_2)\left(1 - \phi_1 + \phi_1\left(\frac{\rho_{s_1}}{\rho_f}\right)\right) + \phi_2\left(\frac{\rho_{s_2}}{\rho_f}\right),$$

- The electrical conductivities are given by

$$\frac{\sigma_{hnf}}{\sigma_f} = \frac{\sigma_{s_2} + 2\sigma_{bf} + 2\phi_2(\sigma_{s_2} - \sigma_f)}{\sigma_{s_2} + 2\sigma_{bf} - \phi_2(\sigma_{s_2} - \sigma_f)}$$

where

$$\frac{\sigma_{bf}}{\sigma_f} = \frac{\sigma_{s_1} + 2\sigma_f + 2\phi_1(\sigma_{s_1} - \sigma_f)}{\sigma_{s_1} + 2\sigma_f - \phi_1(\sigma_{s_1} - \sigma_f)},$$

Table 2. Comparison of the $-f''(0)$values with the previous study by varying M and $\phi_1 = \phi_2 = \Lambda = Da^{-1} = d = L = S = 0$.

M	Yih (1999)	Present results
0.0	−1.0000	−1.00000
0.5	−1.2247	−1.22412
1.0	−1.4142	−1.41414
1.5	−1.5811	−1.58122
2.0	−1.7321	−1.73299

- Thermal capacitance of the hybrid nanofluid quantity as follows:

$$\frac{(\rho C_p)_{hnf}}{(\rho C_p)_f} = (1-\phi_2) \times \left(1 - \phi_1 + \phi_1 \left(\frac{(\rho C_P)_{s_1}}{(\rho C_P)_f}\right)\right) + \phi_2 \left(\frac{(\rho C_P)_{s_2}}{(\rho C_P)_f}\right),$$

- Thermal conductivity of hybrid nanofluid quantity as follows:

$$\frac{\kappa_{hnf}}{\kappa_f} = \frac{\kappa_{s_2} + 2\kappa_{bf} + 2\phi_2(\kappa_{s_2} - \kappa_f)}{\kappa_{s_2} + 2\kappa_{bf} - \phi_2(\kappa_{s_2} - \kappa_f)}$$

where

$$\frac{\kappa_{bf}}{\kappa_f} = \frac{\kappa_{s_1} + 2\kappa_f + 2\phi_1(\kappa_{s_1} - \kappa_f)}{\kappa_{s_1} + 2\kappa_f - \phi_1(\kappa_{s_1} - \kappa_f)},$$

Table 2 depicts the comparison of the present values of the $-f''(0)$with those of Yih (1999) for various numbers of the magnetic parameter. The comparison reveals that the two sets of results are in very close agreement. The maximum percentage error is about 0.05%, which is a clear indication of the high level of accuracy, validity, and dependability of the present analytical formulation and solution method.

3. Results and discussion

The present research examines the force of the Lorentz force and viscosity ratio on ferrohybrid nanofluid motion across an expanding sheet with entropy generation. Fe_3O_4 and CuO nanoparticles are mixed in a base fluid to form a ferrohybrid nanofluid. The considered PDEs are changed to ODEs via suitable similarity variables, the radiation effect is considered in the energy equation and solved using Laguerrel polynomial, and also calculated the entropy generation. Several physical parameters, such as Brinkman number, magnetic field, porosity, radiation, heat source/sink, and Eckert number, are calculated and explained through graphs; thermophysical properties are given in Table 1.

Figure 2(a,b) portrays the impact of mass transpiration on both velocity and temperature profiles. Graphs taken for expanding surface, the physical explanation is that suction at the boundary causes the fluid to be drawn closer to the sheet, reducing the boundary-layer thickness and increasing the shear, which in turn decreases the velocity. The suction brings the fluid at ambient conditions closer to the sheet, reducing boundary-layer thickness. By sucking more air at the surface, the velocity boundary layer becomes thinner since fluid particles are attracted to the sheet, thus restricting the velocity profile. Consequently, this withdrawal of the boundary-layer fluid improves the momentum damping and flow stabilisation.

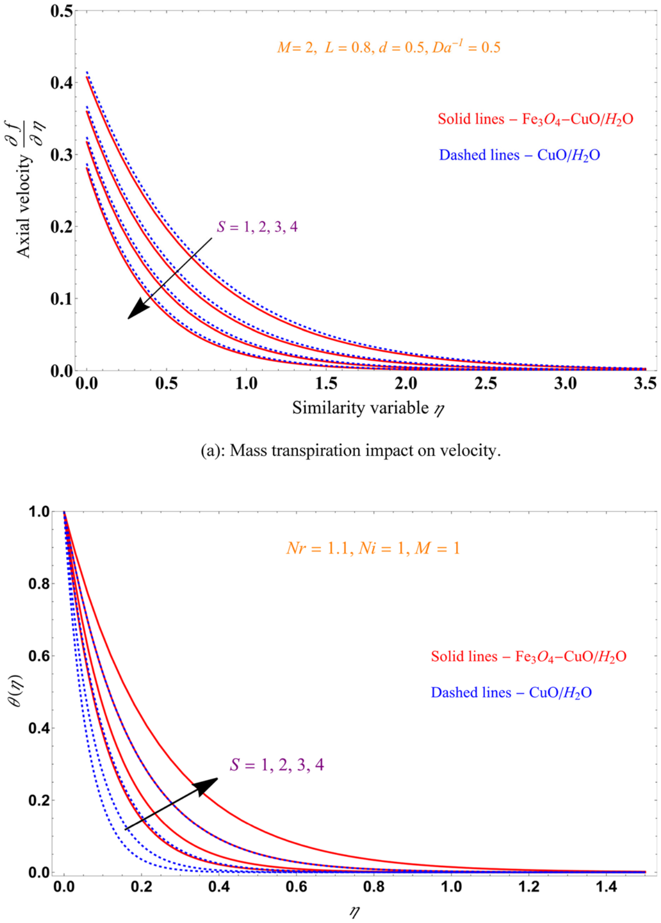

(a): Mass transpiration impact on velocity.

(b): Mass transpiration impact on temperature.

Figure 2. Mass transpiration impact on (a) velocity and (b) temperature.

Figure 3(a,b) portrays the influence of the Da^{-1} on both velocity and skin friction profiles. Graphs are taken for stretching surface; the physical significance is that higher inverse Darcy numbers correspond to greater permeability of the porous medium, which allows for lower fluid velocities at the same pressure gradient, and increasing the Da^{-1} increases the skin friction. Enhancing the porosity parameter means the porous medium being less permeable contributes more resistance to the fluid motion. This extra drag force cuts down the velocity profile by the boundary layer losing momentum. So, the wall shear stress goes up, and the skin friction gets increased.

Figure 4(a,b) represents the impact of the viscosity ratio on both velocity and skin friction profiles. Graphs are taken for stretching surface; the physical explanation is that the viscosity ratio is a dimensionless parameter that denotes the ratio of heat generated by dissipation to energy transported by molecular conduction. It has an important effect on the velocity of the fluid. The influence of improving the viscosity ratio is to decrease the velocity profile; the higher its choices reduce the conduction of heat produced, the greater the increase in energy. This indicates that a higher viscosity ratio tends to a decrease in the velocity profile, and higher Brinkman numbers result in higher skin friction.

Figure 5(a,b) portrays the impact of the velocity slip on both velocity and skin friction profiles. Graphs are taken for stretching surface; an increase in the velocity slip parameter reduces the

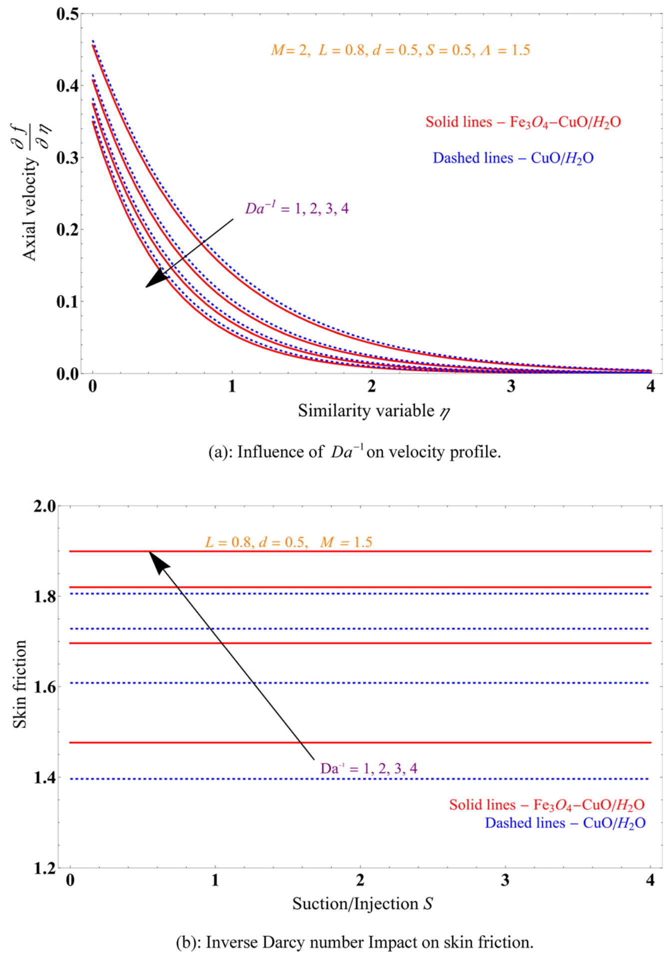

Figure 3. (a) Influence of Da^{-1}on velocity profile and (b) inverse Darcy number Impact on skin friction.

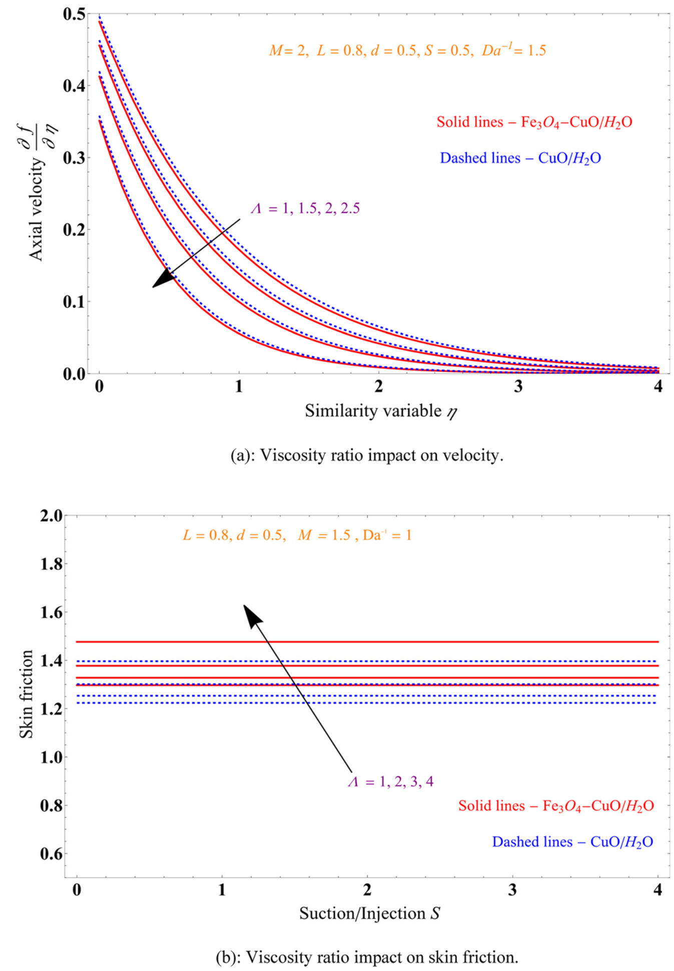

Figure 4. Viscosity ratio impact on (a) velocity and (b) skin friction.

adhesion between the fluid and the stretching sheet, allowing partial relative motion at the wall. As a result, less momentum is transferred from the sheet to the fluid, tends to a reduction in the velocity regime. The diminished momentum exchange also lowers the wall shear stress, thereby decreasing the skin friction coefficient. Physically, slip reduces viscous drag by relaxing the classical no-slip constraint. The slip phenomenon occurs when the velocity of the fluid and the sheet are not the same, which reduces the fluid motion and thus decreases the skin friction and velocity.

Figure 6 represents the influence of the stretching term of the velocity profile. As the stretching parameter increases, the velocity of the nanofluid upsurges. This is because the stretching enhances the nanofluid velocity, which reduces the viscous effects on the flow. An increase in the term d intensifies the sheet velocity, which enhances the movement from the sheet to the fluid. This stronger stretching action accelerates the fluid particles near the wall, thereby increasing the velocity within the boundary layer. Physically, higher stretching rates thin the momentum boundary layer and promote stronger flow alignment along the sheet due to increased shear forcing.

Figure 7(a–e) represents the impact of the magnetic field on velocity, energy, skin friction, Nusselt number, and Eg profiles. Graphs are taken for stretching surface; the physical explanation is that the MHD develops a Lorentz force that restricts the fluid flow; the Lorentz force produced by the MHD restricts the fluid flow, which can reduce the convective energy transfer and affect the temperature profiles; in the presence of a MHD, the concentration of magnetite particles turns the friction surface increases, which can lead to higher skin friction; stronger magnetic field leads to greater flow mixing, which can enhance the energy transfer and increase the Nusselt number; upsurging magnetic felid decreases the entropy generation magnetic field leads to higher shear stresses and flow mixing, which in turn increases irreversibility and entropy production.

Figure 8(a,b) depicts the impact of the heat source on temperature and Nusselt number. Graphs are taken for stretching surface, the physical explanation is that the Nusselt number term is a non-dimensional quantity that relates the convective energy transfer to the conductive energy transfer. The heat source generates more heat energy, causing the fluid temperature to increase and consequently suppress the Nusselt number. Raising the heat source leads to more internal thermal energy being added to the fluid, and as a result, the temperature in the boundary layer improves. When this internal heat is generated, it decreases the temperature gradient at the wall and thus lowers the heat exchange rate. In fact, the heat source can be seen as an energy supply per unit volume that creates a thicker thermal boundary layer and enhances thermal diffusion in the ferrohybrid nanofluid.

Figure 9(a,b) portrays the impact of the radiation on temperature and Nusselt number. Plots are taken for stretching surface;

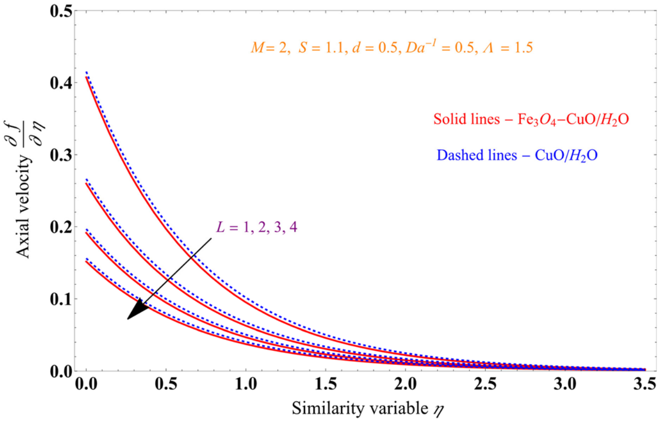

(a): Slip parameter impact on velocity.

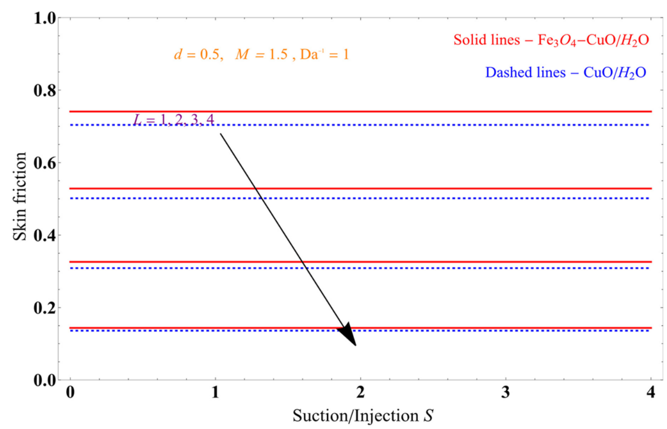

(b): Velocity slip impact on skin friction.

Figure 5. (a) Slip parameter impact on velocity and (b) velocity slip impact on skin friction.

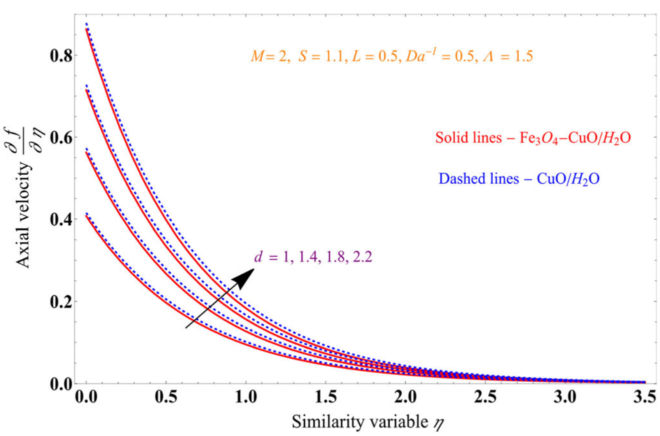

Figure 6. Influence of d on velocity profile.

the physical explanation is that radiation is the fundamental mechanism of energy transfer, along with conduction and convection. It allows energy to be transferred through electromagnetic waves, even in the absence of a medium. Radiation has an increasing effect on the temperature distribution and surface energy of the fluid and decreases the Nusselt number. When the radiation term gets higher, more energy will come to the fluid in the form of radiative heat flux; that is, the energy is supplied to the thermal field. This increase in radiative energy raises the energy distribution and also the boundary layer thickness. From a physical viewpoint, a higher radiation level will lower the local temperature gradient at the wall since the energy is transported more efficiently by the radiative waves; thus, the fluid temperature rises as a whole.

Figure 10(a,b) portrays the impact of the Ec on temperature and entropy generation. Graphs are taken for stretching surface; the physical explanation is that the Eckert term is a non-dimensional term that represents the division of the kinetic energy of the fluid to the enthalpy driving force for heat transfer, as the Eckert number improves it indicates that the viscous dissipation effects become more significant, which enhance the temperature of the fluid flow, higher Eckert numbers correspond to stronger heat dissipation effects, which contribute to greater irreversibility and entropy production.

Figure 11(a) represents the impact of the Br on Eg, and Figure 11(b) represents the porosity impact on entropy generation; the physical explanation is that increasing the Br increases the entropy generation, increasing Br causes friction between fluid layers in the boundary-layer area, resulting in increased heat output. A higher Br value increases the friction force and generates additional energy inside the system, resulting in the rate of entropy formation appearing to grow. The porosity parameter is the main factor that affects entropy in the ferro-hybrid nanofluid flow. When the Da^{-1} increases, it means that the permeability is decreasing. Consequently, the flow resistance is increased, and the viscous friction within the boundary layer becomes stronger. Therefore, fluid friction irreversibility is raised, and thus, entropy production goes up. On a physical basis, lower permeability raises the dissipation of velocity and the conversion of internal energy, which means that there are more thermodynamic losses in the system.

Figure 12(a–e) represents the streamlined graphs of fluid flow; graphs are taken for different choices of the MHD, viscosity ratio, and inverse Darcy number. Streamline graphs are used to visualise the flow of fluids. They represent the path that a particle will follow in a steady flow field, where each tangent to the curve at any point is parallel to the velocity vector of the flow at that point. By analysing streamline patterns, we can determine whether the movement is laminar or turbulent, predict pressure drop in pipes, and optimise equipment design involving fluid flow, like aircraft wings, automotive bodies, or even cardiovascular systems.

4. Conclusion

The current article examines the influence of MHD and viscosity ratio on ferrohybrid nanofluid flow across expanding surfaces with entropy analysis. Fe_3O_4 and CuO nanoparticles are mixed in a base fluid to form a ferrohybrid nanofluid. The considered PDEs are changed to ODEs via suitable similarity conversions, radiation, and heat generation included in the temperature equation and solved using Laguerrel polynomial, and also calculated the entropy generation. Several physical terms, such as Brinkman number, MHD, inverse Darcy number, Radiation, Heat source/sink, Eckert number parameters, are calculated and explained through graphs; thermophysical properties are stated in Table 1. The findings of the current study are stated as follows:

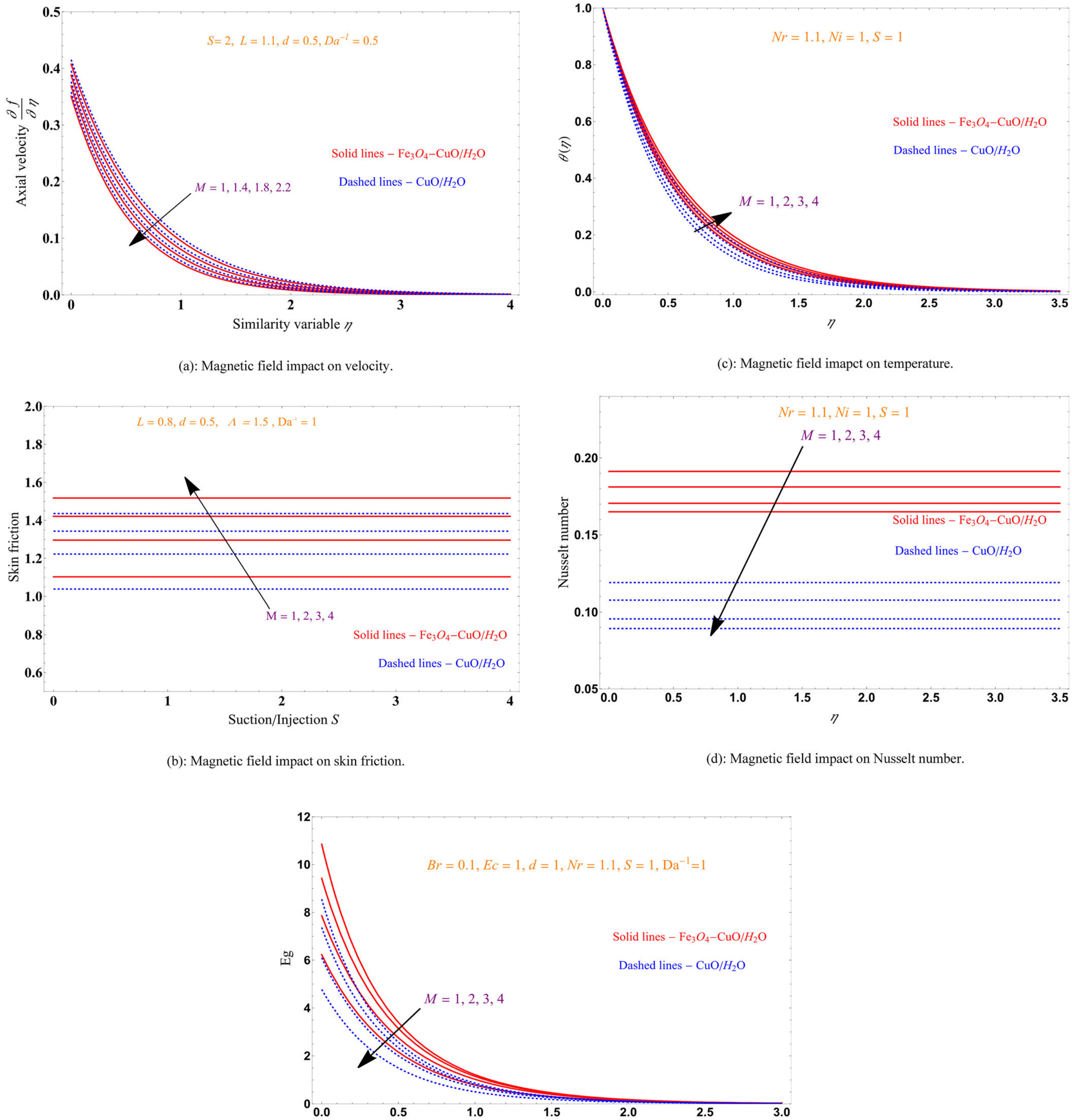

(a): Magnetic field impact on velocity.

(c): Magnetic field imapct on temperature.

(b): Magnetic field impact on skin friction.

(d): Magnetic field impact on Nusselt number.

(e): Magnetic field impact over entropy generation.

Figure 7. Magnetic field impact on (a) velocity and (b) skin friction. (c) temperature, (d) Nusselt number and (e) entropy generation.

- Increasing the mass transpiration decreases the velocity profile and increases the temperature.
- Increasing the inverse Darcy number decreases the velocity and upsurges the skin friction.
- Increasing the magnetic field decreases the entropy generation and upsurges the skin friction and thermal boundary layer of the fluid motion.
- Increasing the viscosity ratio decreases the velocity and upsurges the skin friction.
- Increasing the velocity slip decreases the velocity and skin friction.
- Increasing the heat source term decreases the Nusselt number.
- Increasing the Eckert raises the temperature and entropy generation.
- Increasing the radiation term upsurges the temperature of the fluid flow and decreases the Nusselt number.

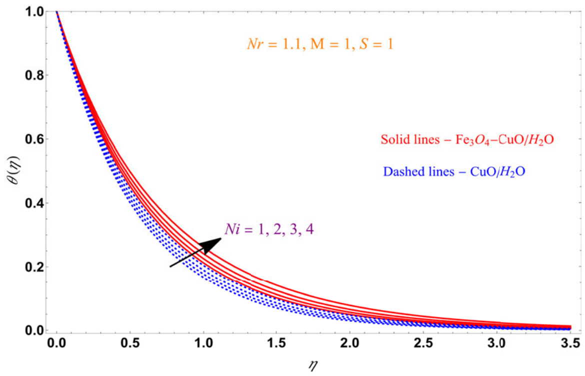

(a): Influence of heat source on temperature.

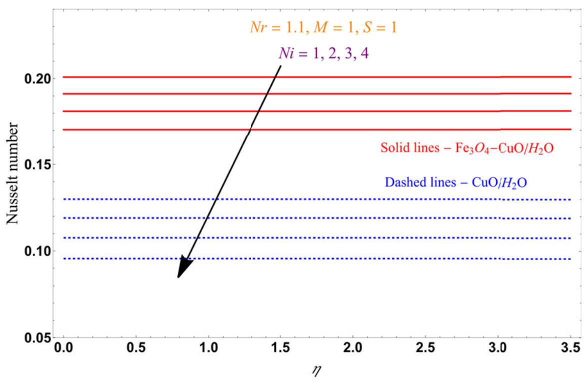

(b): Influence of heat source on Nusselt number.

Figure 8. Influence of heat source on (a) temperature and (b) Nusselt number.

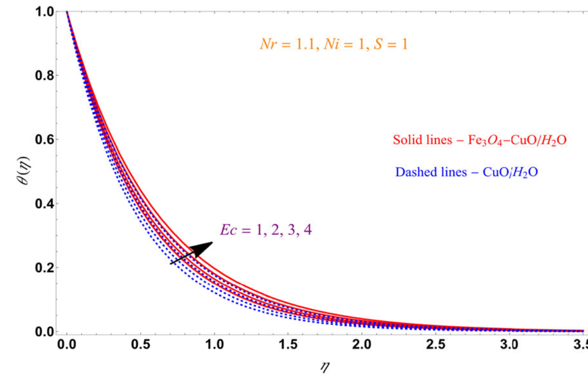

(a): Ec impact on temperature.

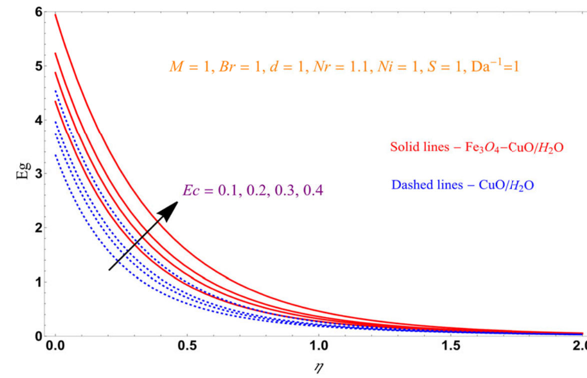

(b): Ec impact on entropy generation.

Figure 10. Ec impact on (a) temperature and (b) entropy generation.

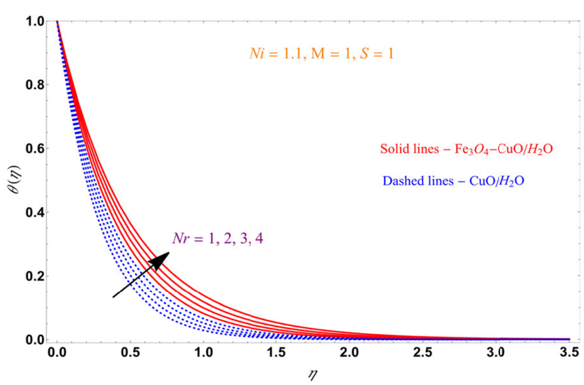

(a): Radiation impact on temperature.

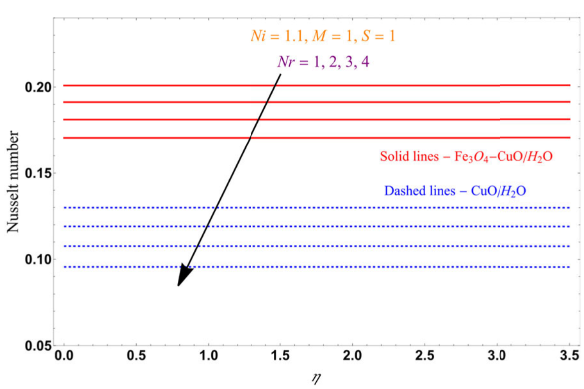

(b): Influence of radiation on Nusselt number.

Figure 9. (a) Radiation impact on temperature and (b) influence of radiation on Nusselt number.

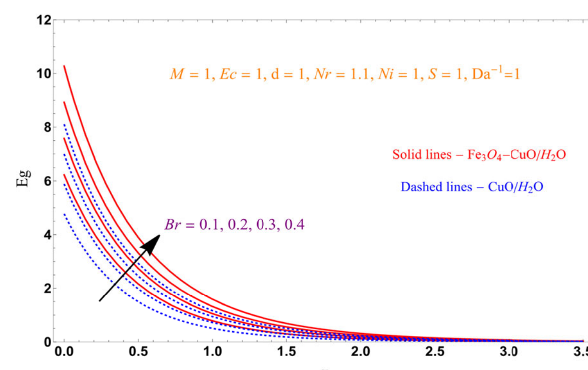

(a): Brinkman number impact on entropy generation.

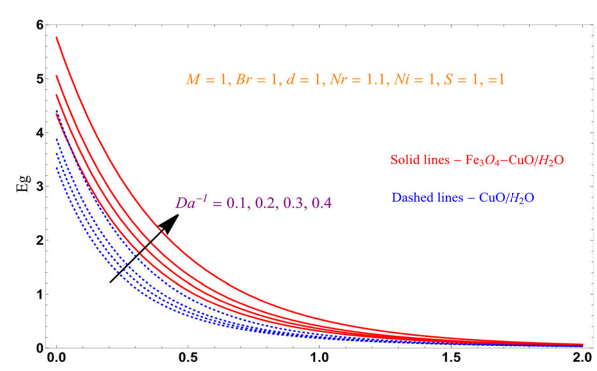

(b): Inverse Darcy number impact on entropy generation.

Figure 11. (a) Brinkman number impact on entropy generation and (b) inverse Darcy number impact on entropy generation.

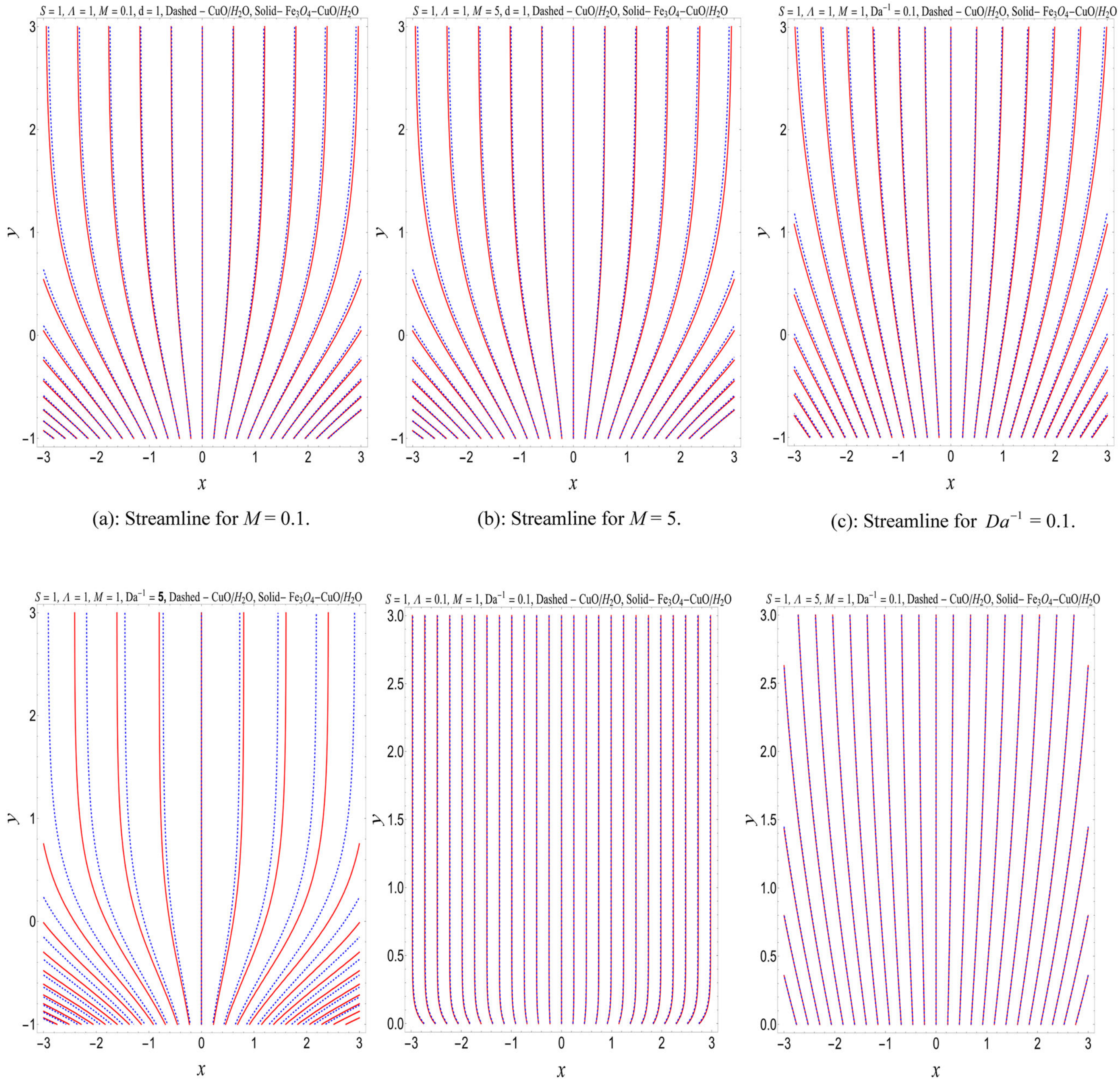

(a): Streamline for $M = 0.1$. (b): Streamline for $M = 5$. (c): Streamline for $Da^{-1} = 0.1$.

(d): Streamline for $Da^{-1} = 5$. (e): Streamline for $\Lambda = 0.1$. (f): Streamline for $\Lambda = 5$.

Figure 12. (a) Streamline for $M = 0.1$, (b) $M = 5$, (c) $Da^{-1} = 0.1$, (d) $Da^{-1} = 5$, (e) $\Lambda = 0.1$, and (f) $\Lambda = 5$.

The current study has many useful applications in polymer extrusion processes and cooling systems, and medical and industrial applications. The present problem can be extended by adding thermal jump and additional nanoparticles, effects of micropolar, and Williamson fluids over various boundaries such as convergent/divergent channels, Riga plate, cone, wedge and inclined surface.

Acknowledgement

Dr. Sachhin S. M. sincerely thanks the University of Tarapacá (Chile) for the kind invitation and generous hospitality extended to him as a visiting scholar through the Visiting Researchers Program during the academic year 2025–2026. He expresses his deep gratitude to his research supervisor, Professor U. S. Mahabaleshwar, for his constant guidance and support, and also extends sincere thanks to Prof. David Laroze (Universidad de Tarapacá) for his warm hospitality and valuable assistance during his visit.

Author contributions

CRediT: **S.M. Sachhin:** Conceptualization, Formal analysis, Investigation, Methodology, Resources, software, Validation, Writing – original draft, Writing – review & editing; **U.S. Mahabaleshwar:** Conceptualization, Data curation, Funding acquisition, Project administration, Software, Supervision, Validation, Writing – original draft, Writing – review & editing; **David Laroze:** Conceptualization, Data curation, Formal analysis, Funding acquisition, Investigation, Project administration, Supervision, Validation, Visualization; **L. M. Pérez:** Conceptualization, Data curation, Formal analysis, Funding acquisition, Investigation, Resources, Software, Supervision, Validation, Visualization

Disclosure statement

No potential conflict of interest was reported by the authors.

Data availability statement

Data sharing is not applicable to this article as no new data were created or analysed in this study.

ORCID

S.M. Sachhin http://orcid.org/0009-0006-4101-1074

References

Ali, A., M. Ahmed, A. Ahmad, and R. Nawaz. October, 2023. "Enhanced Heat Transfer Analysis of Hybrid Nanofluid over a Riga Plate: Incorporating Lorentz Forces and Entropy Generation." *Tribology International* 188:108844. https://doi.org/10.1016/j.triboint.2023.108844.

Ali, A., Z. Shah, S. Mumraiz, P. Kumam, and M. Awais. 2019. "Entropy Generation on MHD Peristaltic Flow of Cu-Water Nanofluid with Slip Conditions." *Heat Transfer—Asian Research* 48 (8): 4301–4319. https://doi.org/10.1002/htj.21593.

Awais, M., T. Hayat, N. Muqaddass, A. Ali, Aqsa, and S. E.Awan. March, 2018. "Nanoparticles and Nonlinear Thermal Radiation Properties in the Rheology of Polymeric Material." *Results in Physics* 8:1038–1045. https://doi.org/10.1016/j.rinp.2018.01.041.

Awais, M., P. Kumam, Memoona, A.Ali, Z.Shah, and H.Alrabaiah. February, 2021. "Impact of Activation Energy on Hyperbolic Tangent Nanofluid with Mixed Convection Rheology and Entropy Optimization." *Alexandria Engineering Journal* 60 (1): 1123–1135. https://doi.org/10.1016/j.aej.2020.10.036.

Barna, I. F., G. Bognár, M. Guedda, L. Mátyás, and K. Hriczó. March, 2020. "Analytic Self-similar Solutions of the Kardar-Parisi-Zhang Interface Growing Equation with Various Noise Terms." *Mathematical Modelling and Analysis* 25 (2): 241–256. https://doi.org/10.3846/mma.2020.10459.

Bèg, ÒÀ, H. S. Takhar, and V. M. Soundalgekar. January, 1998. "Thermoconvective Flow in a Saturated, Isotropic, Homogeneous Porous Medium Using Brinkman's Model: Numerical Study." *International Journal of Numerical Methods for Heat & Fluid Flow* 8 (5): 559–589. https://doi.org/10.1108/09615539810220298.

Bhattacharyya, K., S. Mukhopadhyay, G. C. Layek, and I. Pop. May, 2012. "Effects of Thermal Radiation on Micropolar Fluid Flow and Heat Transfer over a Porous Shrinking Sheet." *International Journal of Heat and Mass Transfer* 55 (11): 2945–2952. https://doi.org/10.1016/j.ijheatmasstransfer.2012.01.051.

Bognár, G. June, 2012. "On Similarity Solutions of Boundary Layer Problems with Upstream Moving Wall in non-newtonian Power-law Fluids." *IMA Journal of Applied Mathematics* 77 (4): 546–562. https://doi.org/10.1093/imamat/hxr033.

Cuce, E., P. M. Cuce, T. Guclu, and A. B. Besir. June, 2020. "On the Use of Nanofluids in Solar Energy Applications." *Journal of Thermal Science* 29 (3): 513–534. https://doi.org/10.1007/s11630-020-1269-3.

Cuce, E., T. Guclu, and P. M. Cuce. June, 2020. "Improving Thermal Performance of Thermoelectric Coolers (TECs) through a Nanofluid Driven Water to air Heat Exchanger Design: An Experimental Research." *Energy Conversion and Management* 214:112893. https://doi.org/10.1016/j.enconman.2020.112893.

Cunha, F. R., and Y. D. Sobral. November, 2004. "Characterization of the Physical Parameters in a Process of Magnetic Separation and Pressure-Driven Flow of a Magnetic Fluid." *Physica A: Statistical Mechanics and Its Applications* 343:36–64. https://doi.org/10.1016/j.physa.2004.04.122.

CÜCE, A., T. GÜÇLÜ, and E. Cuce. September, 2022. "The Effect of Nanofluid Usage on Electricity Consumption in Thermoelectric Refrigeration Application: An Experimental Study." *Gazi Journal of Engineering Sciences* 8:228–236. https://doi.org/10.30855/gmbd.0705006.

Dukhan, N., M. A. Al-Rammahi, and A. S. Suleiman. December, 2013. "Fluid Temperature Measurements Inside Metal Foam and Comparison to Brinkman–Darcy Flow Convection Analysis." *International Journal of Heat and Mass Transfer* 67:877–884. https://doi.org/10.1016/j.ijheatmasstransfer.2013.08.055.

Erickson, D., D. Sinton, and D. Li. 2003. "Joule Heating and Heat Transfer in Poly(Dimethylsiloxane) Microfluidic Systems." *Lab on a Chip* 3 (3): 141–149. https://doi.org/10.1039/B306158B.

Hayat, T., A. Shafiq, and A. Alsaedi. January, 2014. "Effect of Joule Heating and Thermal Radiation in Flow of Third Grade Fluid over Radiative Surface." *PLoS One* 9 (1): e83153. https://doi.org/10.1371/journal.pone.0083153.

Huminic, G., and A. Huminic. March, 2020. "Entropy Generation of Nanofluid and Hybrid Nanofluid Flow in Thermal Systems: A Review." *Journal of Molecular Liquids* 302:112533. https://doi.org/10.1016/j.molliq.2020.112533.

Hussain, S., A. Ali, K. Rasheed, A. A. Pasha, S. Algarni, T. Alqahtani, and K. Irshad. December, 2023. "Application of Response Surface Methodology to Optimize MHD Nanofluid Flow over a Rotating Disk with Thermal Radiation and Joule Heating." *Case Studies in Thermal Engineering* 52:103715. https://doi.org/10.1016/j.csite.2023.103715.

Khan, Z., H. U. Rasheed, T. Abbas, D. Baleanu, and K. Sooppy Nisar. March, 2020. "Analysis of Eyring–Powell Fluid Flow Used as a Coating Material for Wire with Variable Viscosity Effect along with Thermal Radiation and Joule Heating." *Crystals* 10 (3): 168. https://doi.org/10.3390/cryst10030168.

Khan, W. A., T. A. Yusuf, F. Mabood, M. K. Siddiq, and S. A. Shehzad. November, 2023. "Chemically Reactive Water-Based Carbon Nanotubes Flow Saturated in Darcy-Forchheimer Porous Media Coupled with Entropy Generation." *Chemical Physics Letters* 830:140808. https://doi.org/10.1016/j.cplett.2023.140808.

Klazly, M., and G. Bognár. June, 2022. "A Novel Empirical Equation for the Effective Viscosity of Nanofluids Based on Theoretical and Empirical Results." *International Communications in Heat and Mass Transfer* 135:106054. https://doi.org/10.1016/j.icheatmasstransfer.2022.106054.

Kumar, R. N., F. Gamaoun, A. Abdulrahman, J. S. Chohan, and R. J. P. Gowda. October, 2022. "Heat Transfer Analysis in Three-Dimensional Unsteady Magnetic Fluid Flow of Water-Based Ternary Hybrid Nanofluid Conveying Three Various Shaped Nanoparticles: A Comparative Study." *International Journal of Modern Physics B* 36 (25): 2250170. https://doi.org/10.1142/S0217979222501703.

Li, Y. B., Z. Q. Lin, S. J. Hu, and G. L. Chen. March, 2007. "Numerical Analysis of Magnetic Fluid Dynamics Behaviors during Resistance Spot Welding." *Journal of Applied Physics* 101 (5): 053506. https://doi.org/10.1063/1.2472279.

Li, Q., and Y. Xuan. April, 2009. "Experimental Investigation on Heat Transfer Characteristics of Magnetic Fluid Flow around a Fine Wire under the Influence of an External Magnetic Field." *Experimental Thermal and Fluid Science* 33 (4): 591–596. https://doi.org/10.1016/j.expthermflusci.2008.12.003.

Liu, W. I., J. Alsarraf, A. Shahsavar, M. Rostamzadeh, M. Afrand, and T. K. Nguyen. August, 2019. "Impact of Oscillating Magnetic Field on the Thermal-Conductivity of Water-Fe3O4 and Water-Fe3O4/CNT Ferro-Fluids: Experimental Study." *Journal of Magnetism and Magnetic Materials* 484:258–265. https://doi.org/10.1016/j.jmmm.2019.04.042.

Lone, S. A., F. Ali, A. Saeed, and G. Bognár. April, 2023. "Irreversibility Analysis with Hybrid Cross Nanofluid of Stagnation Point and Radiative Flow (TiO_2+CuO) Based on Engine oil Past a Stretchable Sheet." *Heliyon* 9 (4): e15056. https://doi.org/10.1016/j.heliyon.2023.e15056.

Mabood, F., T. A. Yusuf, and G. Bognár. November, 2020. "Features of Entropy Optimization on MHD Couple Stress Nanofluid Slip Flow with Melting Heat Transfer and Nonlinear Thermal Radiation." *Scientific Reports* 10 (1): 19163. https://doi.org/10.1038/s41598-020-76133-y.

Mahabaleshwar, U. S., S. M. Sachhin, L. M. Pérez, and G. Lorenzini. September, 2024. "An Effect of Mass Transpiration and Darcy–Brinkman Model on Ostwald–de Waele Ternary Nanofluid." *Journal of Engineering Thermophysics* 33 (3): 547–565. https://doi.org/10.1134/S181023282403010X.

Mansourian, M., S. Dinarvand, and I. Pop. June, 2022. "Aqua Cobalt Ferrite/Mn–Zn Ferrite Hybrid Nanofluid Flow over a Nonlinearly Stretching Permeable Sheet in a Porous Medium." *Journal of Nanofluids* 11 (3): 383–391. https://doi.org/10.1166/jon.2022.1841.

Megahed, A. M., M. G. Reddy, and W. Abbas. July, 2021. "Modeling of MHD Fluid Flow over an Unsteady Stretching Sheet with Thermal Radiation, Variable Fluid Properties and Heat Flux." *Mathematics and Computers in Simulation* 185:583–593. https://doi.org/10.1016/j.matcom.2021.01.011.

Mehrali, M., E. Sadeghinezhad, A. R. Akhiani, S. Tahan Latibari, H. S. C. Metselaar, and A. S. Kherbeet. February, 2017. "Heat Transfer and Entropy Generation Analysis of Hybrid Graphene/Fe3O4 Ferro-Nanofluid Flow under the Influence of a Magnetic Field." *Powder Technology* 308:149–157. https://doi.org/10.1016/j.powtec.2016.12.024.

Minale, M. February, 2016. "Modelling the Flow of a Second Order Fluid through and over a Porous Medium Using the Volume Averages. I. The Generalized Brinkman's Equation." *Physics of Fluids* 28 (2): 023102. https://doi.org/10.1063/1.4941575.

Mumraiz, S., A. Ali, M. Awais, M. Shutaywi, and Z. Shah. February, 2021. "Entropy Generation in Electrical Magnetohydrodynamic Flow of Al2O3–Cu/H2O Hybrid Nanofluid with non-uniform Heat Flux." *Journal of Thermal Analysis and Calorimetry* 143 (3): 2135–2148. https://doi.org/10.1007/s10973-020-09603-0.

Nield, D. A. March, 1983. "The Boundary Correction for the Rayleigh-Darcy Problem: Limitations of the Brinkman Equation." *Journal of Fluid Mechanics* 128:37–46. https://doi.org/10.1017/S0022112083000361.

Pramanik, S. March, 2014. "Casson Fluid Flow and Heat Transfer Past an Exponentially Porous Stretching Surface in Presence of Thermal Radiation." *Ain Shams Engineering Journal* 5 (1): 205–212. https://doi.org/10.1016/j.asej.2013.05.003.

Qureshi, M. Z. A., Q. Raza, S. M. Eldin, M. Zafar, B. Ali, and I. Siddique. January, 2023. "Thermal Performance of Hybrid Magnetized Nanofluids Flow Subject to Joint Impact of Ferro Oxides/CNT Nanomaterials with Radiative and Porous Factors." *Case Studies in Thermal Engineering* 41:102648. https://doi.org/10.1016/j.csite.2022.102648.

Radionov, A., A. Podoltsev, and A. Zahorulko. January, 2012. "Finite-Element Analysis of Magnetic Field and the Flow of Magnetic Fluid in the Core of Magnetic-Fluid Seal for Rotational Shaft." *Procedia Engineering* 39:327–338. https://doi.org/10.1016/j.proeng.2012.07.038.

Sachhin, S. M., P. K. Ankitha, G. M. Sachin, U. S. Mahabaleshwar, I. V. Shevchuk, S. N. R. Nayakar, and R. Kadli. December, 2024. "Chemically Reactive Micropolar Hybrid Nanofluid Flow over a Porous Surface in the Presence of an Inclined Magnetic Field and Radiation with Entropy Generation." *Physics* 6 (4): 1315–1344. https://doi.org/10.3390/physics6040082.

Sachhin, S. M., M. S. Bharath, U. S. Mahabaleshwar, G. V. Bognar, and L. M. Pérez. January, 2026. "Dual Modeling of Unsteady Radiative non-newtonian Fluid Flow with Biot Boundary Conditions Using Novel Time-Dependent Solutions." *Mechanics of Time-Dependent Materials* 30 (1): 5. https://doi.org/10.1007/s11043-025-09849-x.

Sachhin, S. M., F.-J. Granados-Ortiz, U. S. Mahabaleshwar, J. Ortega-Casanova, and L. M. Pérez. October, 2025. "Heat and Mass Transfer Analysis of a Bingham Ternary Nanofluid Exposed to Radiation over Stretching/Shrinking Sheets and Stefan Blowing Effect." *Alexandria Engineering Journal* 129:515–529. https://doi.org/10.1016/j.aej.2025.06.026.

Sachhin, S. M., U. S. Mahabaleshwar, D. Laroze, and L. M. Pérez. November, 2025. "Exact Multiple Solutions for Rheological Analysis of Darcy–Brinkman Model on Bingham Sodium Alginate Suspensions Driven by 2D Bidirectional Moving Plate with Navier and Biot Conditions." *Journal of Thermal Analysis and Calorimetry* 150 (22): 18327–18344. https://doi.org/10.1007/s10973-025-14693-9.

Sachhin, S. M., U. S. Mahabaleshwar, N. Swaminathan, L. M. Pérez, and J. Wang. March, 2025. "Thermal Dynamics and Magnetohydrodynamics in Ferrofluidic Wall jet Flow: Entropy Generation in Heat and Mass Transfer." *Journal of Molecular Liquids* 427:127449. https://doi.org/10.1016/j.molliq.2025.127449.

Salawu, S., O. Hammed, T. Yusuf, R. Lebelo, and R. Mustapha. July, 2023. "Entropy Generation in a Magnetohydrodynamic Hybrid Nanofluid Flow over a Nonlinear Permeable Surface with Velocity Slip Effect." *Wseas Transactions on Fluid Mechanics* 18:34–48. https://doi.org/10.37394/232013.2023.18.4.

Sarma, R., and P. K. Mondal. January, 2018. "Entropy Generation Minimization in a Pressure-Driven Microflow of Viscoelastic Fluid with Slippage at the Wall: Effect of Conjugate Heat Transfer." *Journal of Heat Transfer* 140:052402. https://doi.org/10.1115/1.4038451.

Shah, F., M. I. Khan, T. Hayat, M. I. Khan, A. Alsaedi, and W. A. Khan. December, 2019. "Theoretical and Mathematical Analysis of Entropy Generation in Fluid Flow Subject to Aluminum and Ethylene Glycol Nanoparticles." *Computer Methods and Programs in Biomedicine* 182:105057. https://doi.org/10.1016/j.cmpb.2019.105057.

Shojaeian, M., and A. Koşar. March, 2014. "Convective Heat Transfer and Entropy Generation Analysis on Newtonian and non-newtonian Fluid Flows between Parallel-Plates under Slip Boundary Conditions." *International Journal of Heat and Mass Transfer* 70:664–673. https://doi.org/10.1016/j.ijheatmasstransfer.2013.11.020.

Singh, P. K., K. B. Anoop, T. Sundararajan, and S. K. Das. October, 2010. "Entropy Generation due to Flow and Heat Transfer in Nanofluids." *International Journal of Heat and Mass Transfer* 53 (21): 4757–4767. https://doi.org/10.1016/j.ijheatmasstransfer.2010.06.016.

Sridharan, S., J. Zhu, G. Hu, and X. Xuan. 2011. "Joule Heating Effects on Electroosmotic Flow in Insulator-Based Dielectrophoresis." *ELECTROPHORESIS* 32 (17): 2274–2281. https://doi.org/10.1002/elps.201100011.

Srinivasacharya, D., and K. Hima Bindu. June, 2016. "Entropy Generation in a Micropolar Fluid Flow through an Inclined Channel." *Alexandria Engineering Journal* 55 (2): 973–982. https://doi.org/10.1016/j.aej.2016.02.027.

Syam Sundar, L., M. K. Singh, M. C. Ferro, and A. C. M. Sousa. May, 2017. "Experimental Investigation of the Thermal Transport Properties of Graphene Oxide/Co3O4 Hybrid Nanofluids." *International Communications in Heat and Mass Transfer* 84:1–10. https://doi.org/10.1016/j.icheatmasstransfer.2017.03.001.

Tang, G. Y., C. Yang, J. C. Chai, and H. Q. Gong. January, 2004. "Joule Heating Effect on Electroosmotic Flow and Mass Species Transport in a Microcapillary." *International Journal of Heat and Mass Transfer* 47 (2): 215–227. https://doi.org/10.1016/j.ijheatmasstransfer.2003.07.006.

Tsay, R.-Y., and S. Weinbaum. May, 1991. "Viscous Flow in a Channel with Periodic Cross-Bridging Fibres: Exact Solutions and Brinkman Approximation." *Journal of Fluid Mechanics* 226:125–148. https://doi.org/10.1017/S0022112091002318.

Yang, J., Z. Abdelmalek, N. Muhammad, and M. T. Mustafa. November, 2020. "Hydrodynamics and Ferrite Nanoparticles in Hybrid Nanofluid." *International Communications in Heat and Mass Transfer* 118:104883. https://doi.org/10.1016/j.icheatmasstransfer.2020.104883.

Yao, W., Z. Shen, and G. Ding. November, 2013. "Simulation of Interstitial Fluid Flow in Ligaments: Comparison among Stokes, Brinkman and Darcy Models." *International Journal of Biological Sciences* 9 (10): 1050–1056. https://doi.org/10.7150/ijbs.7242.

Yih, K. A. 1999. "Free Convection Effect on MHD Coupled Heat and Mass Transfer of a Moving Permeable Vertical Surface." *International Communications in Heat and Mass Transfer* 26:95–104. https://doi.org/10.1016/S0735-1933(98)00125-0

Yu, D., and R. Wang. January, 2022. "An Optimal Investigation of Convective Fluid Flow Suspended by Carbon Nanotubes and Thermal Radiation Impact." *Mathematics* 10 (9): 1542. https://doi.org/10.3390/math10091542.

Yusuf, T. A. August, 2024. "Entropy Analysis of Unsteady MHD Nanofluid Flow over a Stretching Surface with Effects of Variable Viscosity and Nonuniform Heat Generation." *Numerical Heat Transfer, Part A: Applications* 85 (16): 2754–2771. https://doi.org/10.1080/10407782.2023.2229011.

Yusuf, T. A. December, 2023. "Analysis of Entropy Generation in Nonlinear Convection Flow of Unsteady Magneto-Nanofluid Configured by Vertical Stretching Sheet with Ohmic Heating." *International Journal of Ambient Energy* 44 (1): 2319–2335. https://doi.org/10.1080/01430750.2023.2236103.

Zhao, C., and C. Yang. March, 2012. "Joule Heating Induced Heat Transfer for Electroosmotic Flow of Power-law Fluids in a Microcapillary." *International Journal of Heat and Mass Transfer* 55 (7): 2044–2051. https://doi.org/10.1016/j.ijheatmasstransfer.2011.12.005.